

# Elimination of spiral waves in a one-layer and two-layer network of Pancreatic $\beta$ cells using a periodic stimuli

Karthikeyan Rajagopal<sup>a,\*</sup>, Zhouchao Wei<sup>c</sup>, Irene Moroz<sup>d</sup>, Anitha Karthikeyan<sup>a</sup>, Prakash Duraisamy<sup>b</sup>

<sup>a</sup>Nonlinear Systems and Applications, Faculty of Electrical and Electronics Engineering, Ton Duc Thang University, Ho Chi Minh City, Vietnam.

<sup>b</sup>Center for Nonlinear Dynamics and Control, Mekelle University, Ethiopia.

<sup>c</sup>School of Mathematics and Physics, China University of Geosciences, Wuhan, China.

<sup>d</sup>Mathematical Institute, University of Oxford, Andrew Wiles Building, Oxford, UK.

\* karthikeyan.rajagopal@tdtu.edu.vn, rkarthikeyan@gmail.com

## Abstract

Regulating the glucose level in human body is achieved through the Pancreatic  $\beta$  cells and the glucose release is mainly governed by the bursting activity of the  $\beta$  cells. The Pernarowski model is one of the well known Pancreatic model and is analogous to some of the well known neuron models. The Pernarowski model exhibits chaotic spiking and periodic bursting. In this paper we investigate the dynamical properties of the model through various tools like stability of equilibrium, Hopf's bifurcation, Lyapunov exponents and bifurcation diagrams. As was discussed in literatures the neuron models exhibit spiral waves and so we are interested in understanding such spiral wave generation in the Pernarowski model. For this we construct One-layer and Two-layer network of  $\beta$  cells and study the impact of the plane waves on the spiral wave existence. We show that by a selection of the amplitude and frequency of the stimuli, we can eliminate the spiral waves in the both One-layer and Two-layer network of  $\beta$  cells.

*Keywords:*  $\beta$  cells; chaotic spiking; bifurcation; spiral waves;

## 1. Introduction

**Modeling Pancreatic  $\beta$ -cells** and study of its dynamical behavior, find its attraction on theoretical as well as experimental science for many decades. It plays an important role for insulin secretion that most cells require for glucose metabolism. The dysfunction of pancreatic  $\beta$  cells causes metabolic disorder and leads to diabetes mellitus finally resulted with organ damage [1]. Based on the progressive failure of  $\beta$ -cells, diabetes can be classified in to two major categories type 1 and type 2 respectively. The type 1 diabetes can be identified an autoimmune assault against the  $\beta$ -cells [2-6]. The pathogenesis of type 2 diabetes comprising different degrees of  $\beta$ -cell failure relative to varying degrees of insulin resistance. The endocrine pancreatic  $\beta$ -cells generates insulin in unique pulses as a result of bursting oscillations in membrane potentials. Generally isolated  $\beta$ -cells reported with fast bursting oscillations, while electrically coupled  $\beta$ -cells inside the pancreatic islets shows comparatively slower bursting mode, which is firmly believed to control the amount of insulin secretion and maintain glucose concentration in the blood. The potential of these cells may undergo a transition from bursting, spiking oscillations to continuous spiking oscillations, with

the intervention of stimulatory level of glucose [7-9]. Pancreatic  $\beta$ -cells hold intricate dynamical behavior, among the complex characteristics, Bursting phenomena is studied widely due to its relation to release of insulin [10]. Bursting an observable in a system consists of a periodic succession of silent and active phases [10-12]. Loppini and Pedersen [13] discussed phantom bursting, which depends only on electrical coupling between cells and no changes in parameters. Similarly gap-junction coupling itself can extend the period of bursting upto tenfold, it gives the need for studying the large difference in oscillation frequency between isolated and coupled  $\beta$ -cells. The stable steady state behavior is identified as a silent phase and the rapid oscillation as an active phase. The electrical behavior of single  $\beta$  cells investigated and categorized based on the burst period [14,20]. In order to analyze the dynamical nature of such systems, various mathematical model were developed. Rinzel [19] evaluated the dynamics of the variables during the shifting between these two situations. Based on FitzHugh-Nagumo model [20] a simplified polynomial equation is formulated to depict the biophysical models of bursting electrical activity in pancreatic  $\beta$  cells known as Pernarowski model [16]. Since it is in perturbed Hamiltonian form, Melnikov's method [21] can be implemented to analyze homoclinic bifurcations. In 2016, Fallah [25] studied Pernarowski model during transition between silent phases and continuous spiking, Remarkable dynamical behaviors such as period doubling cascades of canards, chaos and mixed-mode oscillations were found. Symmetric bursting behaviors of fold/super-Hopf type were also discussed. Izhikevich [15] discussed the influence of excitation, its possible bifurcations and their significance in the computational study of neurons.

More importantly, synchronization of electrical impulse bursting and metabolic oscillations needs attention because these are associated with electrical coupling between the cells [22]. The periodic bursting on a network of  $\beta$  cells and synchronization has been studied in [25]. The results reveal that the dynamical behavior while in a network is influenced by other factors such as coupling coefficient, coupling strength etc., Such complex nature leads to states of bistability including two stable critical points and transition with two stable limit cycles [17]. The variation in excitation pushes the system into chaos. Hence Mixed-mode oscillations need to be analyzed for better understanding of the influence of synchronization in transition between symmetric bursting to tonic spiking.

Recent developments in mathematical modelling of biological systems such as fractional order method [35,36] and delayed differential equation treatment, lay a platform to analyze the dynamical behaviors and to capture the sensitive and chaotic nature of the system[37,38]. Most of the biological systems works as network, hence synchronization behavior such as chimera and spiral waves generation and its control needs to be studied thoroughly.

The Spiral wave is a particular spatio-temporal pattern that can appear in the complex network when exposes to external excitation [18]. Significant effects are noted for governing the dynamics of the spatially-extended systems, diffusion across space due to cell-to-cell coupling, and excitability and nonlinear ionic currents that move across the cells [32,33]. This ability to become excited and return to an unexcited state not been discussed sufficiently in the literature. In this paper we investigate bifurcation, multistability, the influence of synchronization effects and spatio-temporal dynamical behavior. More importantly we propose a method to eliminate spiral waves by tuning the amplitude of excitation, coupling coefficient

and coupling strength in a lattice network of beta cells. Similarly we show that stimuli amplitude can be tuned to eliminate the spiral waves in a Two-layer network formed by coupling two different lattices.

In this paper, The Pernarowski model of Pancreatic model  $\beta$  cells is discussed for various dynamical and network behaviors. The introductory section covers the significance of pancreatic  $\beta$  cells in glucose level regulations and effects of dysfunctions of such cells. Literatures which discussed the functionality and characteristics of  $\beta$  cells are presented. Contribution of pernarowski model and various literatures especially on dynamical study are discussed. The introduction about the spiral waves and its consequences in intricate systems are explained. The research gap is identified in the Pernarowski model while treated in network. Section 2 discussing the general Pernarowski model and dimensionless equation. Phase portraits of chaotic attractor with its parameter values is presented. Section 3 deals with numerical analysis with time series plot and bifurcation plots corresponding Lyapunov spectrum is presented. Section 4, dealing the Spiral wave generation and its related discussion. Section 5, providing the Spatio temporal behaviors of Pernarowski model while treating as two layer network. Conclusion section giving the interpretation of the results obtained.

## 2. Pernarowski model for Pancreatic $\beta$ cells

Pancreatic  $\beta$  cells are responsible for the secretion of insulin and thus regulate the glucose level. Every  $\beta$  cell releases glucose when bursting happens in them. The insulin release rate from the  $\beta$  cell is directly proportional to the ratio of the duration of the active phase to the overall period [23]. It was Pernarowski who proposed a simple three-dimensional analog model of bursting activities in pancreatic  $\beta$  cells [24]. The Pernarowski model is analogous to the biophysical models of bursting activity in pancreatic beta cells as like the Fitzhugh–Nagumo model of nerve membrane is analogous to Hodgkin–Huxley model.

The Pancreatic  $\beta$  cell model proposed by Pernarowski [24,25] is given by

$$\begin{aligned} \ddot{u} + F(u)\dot{u} + G(u, c) &= -\varepsilon H(u, c) \\ \dot{c} &= \varepsilon H(u, c) \end{aligned} \tag{1}$$

where

$$\begin{aligned} F(u) &= a[(u - \hat{u})^2 - \eta^2] \\ G(u, c) &= c + u^3 - 3(u + 1) \\ H(u, c) &= \beta(u - \bar{u}) - c \end{aligned} \tag{2}$$

And where  $u$  represents the membrane potential of an excitable cell and  $c$  represents a slow changing variable.

The constants  $a, \hat{u}, \eta$  represents the fast system parameters and  $\beta, \bar{u}$  represents parameters of the slow systems.  $\varepsilon$  represents a small singular parameter varying between  $[0,1]$ . The fast system parameters are responsible for the bursting phenomenon and the slow system parameters are responsible for the changes in the oscillatory behaviors created by fast system parameters. For convenience we derive the dimensionless model as.

$$\begin{aligned}\dot{x} &= y \\ \dot{y} &= -F(x)y - G(x, z) - \varepsilon H(x, z) \\ \dot{z} &= \varepsilon H(x, z)\end{aligned}\tag{3}$$

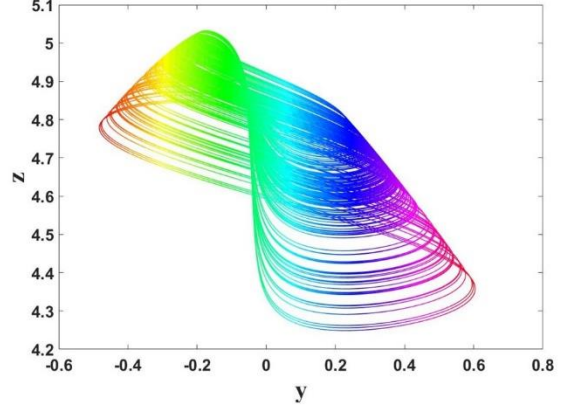
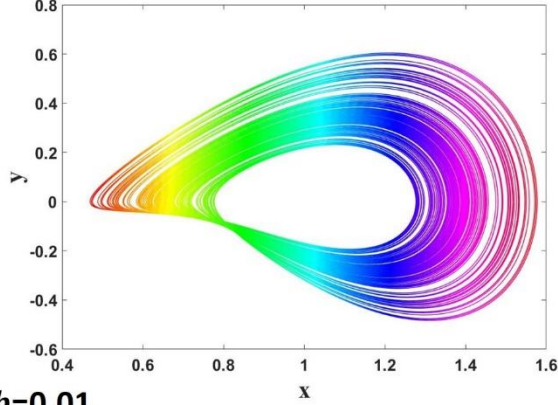
where

$$\begin{aligned}F(x) &= a((x-b)^2 - \eta^2) \\ G(x, z) &= z + x^3 - 3(x+1) \\ H(x, z) &= \beta(x-c) - z;\end{aligned}\tag{4}$$

with the dimensionless variables defined as  $x = u$  and  $c = z$  and parameters are  $b = \hat{u}$  and  $c = \bar{u}$ . The parameters values are

$$a = -0.02, \beta = 2, c = -1.5, \eta = 5.224, \varepsilon = 0.178,\tag{5}$$

**$b=0$**



**$b=0.01$**

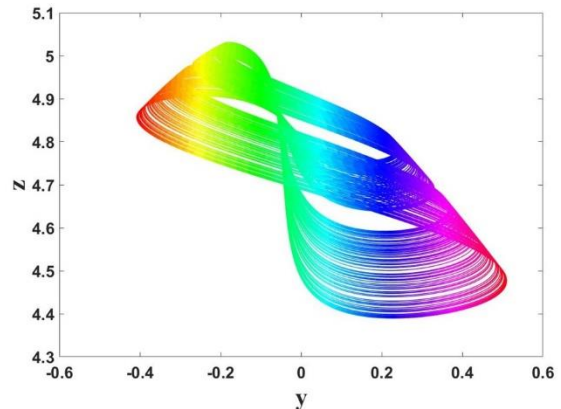
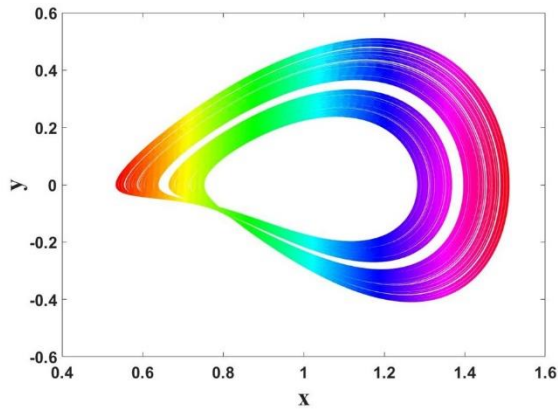


Fig.1: Two-layer Phase portraits of the Pernarowski model for  $b = 0$  (top) and  $b = 0.01$  (bottom)

### 3. Numerical analysis

We First recall the projection method presented in Chapters 3 and 5 [26], but follow the approach of [27-30], used to determine the first Lyapunov coefficient  $l_1$  connected with the stability of a Hopf bifurcation. we consider following differential equation defined by

$$\dot{X} = f(X, \mu), \quad (6)$$

where  $X \in R^3$  and  $\mu \in R^1$  are respectively vectors representing phase variables and control parameters. we assume that  $f$  is a class of  $C^\infty$  in  $R^3 \times R^2$ . Suppose that (6) has an equilibrium  $X = X_0$  at  $\mu = \mu_0$ , and denoting the variable  $X - X_0$  at  $\mu = \mu_0$ , and denoting the variable  $X - X_0$  also by  $X$ , write

$$F(X) = f(X, \mu_0), \quad (7)$$

as

$$F(X) = AX + \frac{1}{2}B(X, X) + \frac{1}{6}C(X, X, X) + o(\|X\|^4), \quad (8)$$

where  $A = f_x(0, \mu_0)$

$$\begin{aligned} B(X, Y) &= \sum_{j,k=1}^3 \frac{\partial^2 F_i(\xi)}{\partial^2 \xi_j \partial \xi_k} \Big|_{\xi=0} X_j Y_k, \\ C(X, Y, Z) &= \sum_{j,k,l=1}^3 \frac{\partial^3 F_i(\xi)}{\partial \xi_j \partial \xi_k \partial \xi_l} \Big|_{\xi=0} X_j Y_k Z_l. \end{aligned} \quad (9)$$

Assume that  $A$  has one pair of complex eigenvalues on the imaginary axis:  $\lambda_{2,3} = \pm i\omega_0$  ( $\omega_0 > 0$ ), and that these eigenvalues are the only eigenvalues with  $\text{Re } \lambda = 0$ . Let  $T^c$  be the generalized eigenvalues of  $A$  corresponding to  $\lambda_{2,3}$ : Let  $p, q \in C^3$  be vectors such that

$$Aq = i\omega_0 q, A^T p = -i\omega_0 p, \langle p, q \rangle = 1, \quad (10)$$

where  $A^T$  is the transpose of the matrix  $A$ , Any vector  $y \in T^c$  can be expressed as  $y = \omega q + \bar{\omega} \bar{q}$ , where  $\omega = \langle p, y \rangle \in C$ . The two-dimensional center manifold related to the eigenvalues  $\lambda_{2,3}$  can be parameterized by  $\omega$  and its complex conjugate  $\bar{\omega}$ , by way of an

immersion of the form  $X = H(\omega, \bar{\omega})$ , where  $H : C^2 \rightarrow R^2$  has a Taylor expansion of the following form

$$H(\omega, \bar{\omega}) = \omega q + \bar{\omega} \bar{q} + \sum_{2 \leq j+k \leq 3} \frac{1}{j!k!} h_{jk} \omega^j \bar{\omega}^k + o(|\omega|^4), \quad (11)$$

with  $h_{jk} \in C^3$  and  $h_{jk} = \bar{h}_{kj}$ . Substituting (11) into (6) and (7) we get the following differential equation

$$H_\omega \omega' + H_{\bar{\omega}} \bar{\omega}' = F(H(\omega, \bar{\omega})), \quad (12)$$

where  $F$  is given by (7). The complex vectors  $H_{ij}$  are determined by the coefficients of (8). Then from the coefficients of  $F$ , system (11) can be written as the following form on the chart  $\omega$  for a central manifold,

$$\dot{\omega} = i\omega_0 \omega + \frac{1}{2} G_{21} \omega |\omega|^2 + o(|\omega|^4), \quad (13)$$

with  $G_{21} \in C$ . The first Lyapunov coefficient can be presented as

$$l_1 = \frac{1}{2} \operatorname{Re} G_{21}, \quad (14)$$

where  $G_{21} = \langle p, C(q, q, \bar{q}), B(\bar{q}, h_{20}) + 2B(q, h_{11}) \rangle$ .

If the Jacobian matrix  $A$  of an equilibrium point has only a pair of purely imaginary eigenvalues  $\pm i\omega_0$  ( $\omega_0 > 0$ ), and the other eigenvalue with nonzero real part, then the equilibrium point undergoes a Hopf bifurcation at  $(X_0, \mu_0)$ . It is clear that a two-dimensional center manifold is well defined at such a Hopf bifurcation point. Also, under the flow generated by (6), it is invariant and any higher-order derivative can be continued to nearby parameter values.

Now we consider the case when  $b = 0$  and the system has three equilibrium points given by

$$A_1 = (0, 0, 3), A_2 = (1, 0, 5), A_3 = (-1, 0, 1). \quad (15)$$

It is not hard to show that there no Hopf bifurcation at  $A_2$  for  $\varepsilon > 0$ . Here, we only consider the Hopf bifurcation of the equilibrium point  $A_2$ , there are analogous results for the equilibrium  $A_3$ . The characteristic equation for the equilibrium  $A_2$  is:

$$\lambda^3 + (0.52580 + \varepsilon) \lambda^2 + 0.52580 \lambda + 2\varepsilon = 0. \quad (16)$$

Suppose that (16) has a pair of imaginary roots  $\pm i\omega$  ( $\omega \in R^+$ ). It is not hard to show that when

$$\varepsilon = \varepsilon_0 \doteq 0.26602. \quad (17)$$

we find the Eigen values to be  $\lambda_1 = -0.79183 < 0, \lambda_{2,3} = \pm 0.81971i$ .

Taking  $\varepsilon$  as the Hopf bifurcation parameter, the transversality condition

$$\text{Re}(\lambda'(\varepsilon_0))|_{\lambda=0.81971i} \approx -0.25865 < 0. \quad (18)$$

is be satisfied. Consequently, we can get the following theorem.

**Theorem 1.1** If  $b$  varies and passes through the critical value  $\varepsilon = \varepsilon_0 \doteq 0.26602$ . system (3) undergoes Hopf bifurcation at equilibrium state  $A_2 = (1, 0, 5)$ .

Here we employ the three dimensional Hopf bifurcation method and symbolic calculations to analyze the parametric variations with respect to dynamic bifurcations. We consider the bifurcation of the system at  $A_2$ .

**Theorem 1.2** The first Lyapunov coefficient related to the equilibrium point  $A_2$  is  $l_1 = -0.29244 < 0$ . Thus the Hopf bifurcation point at the equilibrium state  $A_2$  is supercritical for  $\varepsilon = \varepsilon_0 \doteq 0.26602$ . Moreover, there is an stable limit cycle around the unstable equilibrium point  $A_2$  near  $\varepsilon_0$ .

**Proof** Clearly from (18) the transversality condition is satisfied. Accordingly, a non-degenerated Hopf bifurcation occurs at  $A_2$ . The value of the first Lyapunov coefficient  $l_1$  determines the stability of the bifurcating limit cycle from  $A_2$ . Using the notation of the previous section, the multilinear symmetric functions are given by

$$\begin{aligned} B(x, y) &= (0, 2ab(x_1y_2 + x_2y_1), 0), \quad C(x, y, z) \\ &= (0, -6x_1y_1z_1 - 2a(x_1y_2z_1 + x_2y_1z_1 + x_1y_1z_2), 0). \end{aligned} \quad (19)$$

Furthermore, we can also obtain

$$\begin{aligned} p &= (0.63928 + 0.07453i, 0.29001 + 0.59385i, 0.40483 - 0.39101i), \\ q &= (0.69791, 0.57208i, 0.13300 - 0.40983i) \\ h_{11} &= (0, 0, 0), \\ h_{20} &= (0, 0, 0), \\ G_{21} &= -0.58489 + 1.21446i. \end{aligned} \quad (20)$$

And  $l_1 = -0.29244$ . Therefore, Theorem 1.2 is proved.

Now we choose initial condition  $[1, 0, 4.9]$  and  $\varepsilon=0.265 < \varepsilon_0$ , we eliminate transients, and obtain the stable limit cycle as shown in Fig 2(a). when  $\varepsilon=0.21 < \varepsilon_0$ , we also can obtain another periodic orbit, shown in Fig 2(b). In particular, when  $\varepsilon=0.175 < \varepsilon_0$ , the chaotic orbits are found around equilibria  $A_2$  and  $A_3$  in Fig 2(c) the time series are shown in Fig 2(d).

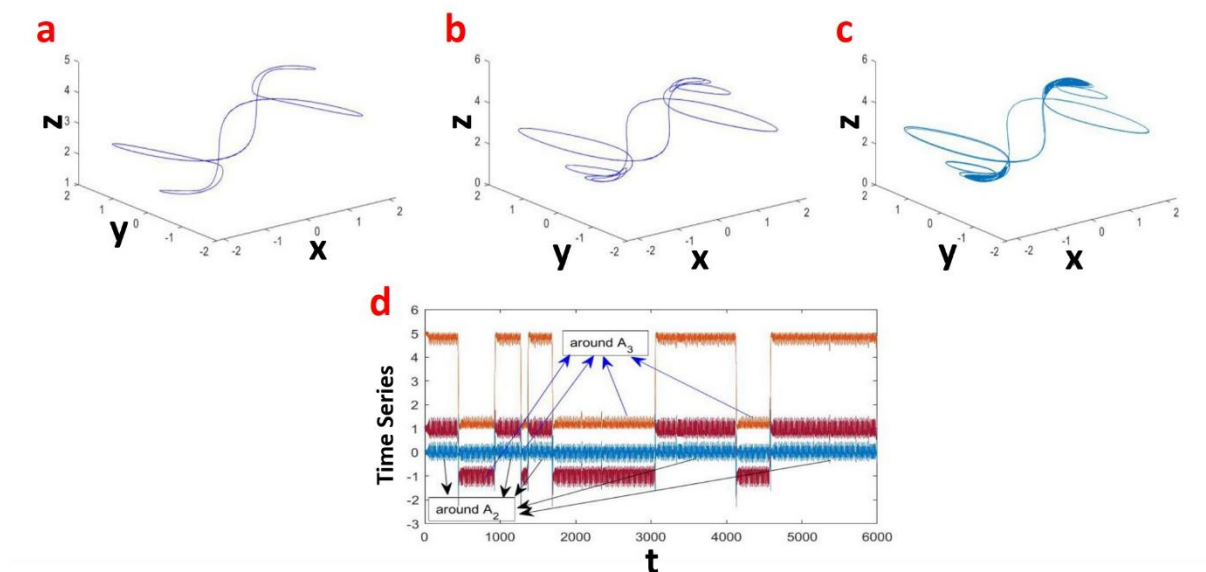


Figure 2: When initial condition  $(1, 0, 4.9)$  system (3) shows periodic orbits and chaotic attractor: (a) periodic orbit from Hopf bifurcation for  $\varepsilon=0.265 < \varepsilon_0$ , (b) periodic orbit for  $\varepsilon=0.21 < \varepsilon_0$ , (c) chaos around equilibria  $A_2$  and  $A_3$  from  $\varepsilon=0.175 < \varepsilon_0$ , (d) time series for  $\varepsilon=0.175 < \varepsilon_0$ .

To understand the dynamical behavior of the system (3) varies with parameter, we derive the bifurcation transition diagram of the system. We choose  $r, b, \eta, \epsilon$  as the control parameters and while the other parameters are kept as in (5). Fig.3 show the bifurcation transition diagram of (3) as  $b$  varies between  $[0, 0.15]$ . We use a fixed initial condition of  $[0.1, 0.1, 0.1]$  to plot the bifurcation diagram. The system undergoes an inverse period doubling exit from chaotic region and we see the chaotic regime for  $b \in [0, 0.03]$ .



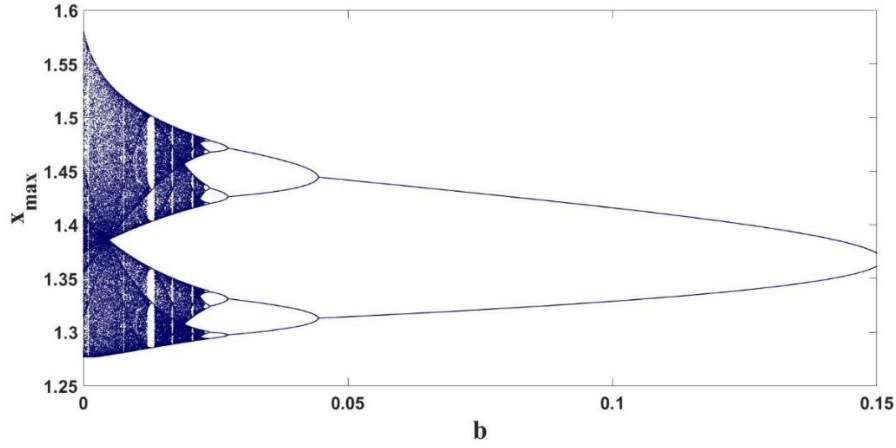


Fig.3: Bifurcation of the system (3) with  $b$

Similarly we can obtain the bifurcation transition plot of the system (3) as  $\epsilon$  varies. The range of  $\epsilon$  is taken between  $[0.16, 0.22]$ . We see several regions showing chaos and the system takes a period doubling route to crisis. We have also plotted the Lyapunov exponents (LEs) of the bifurcation diagram in Fig.4b where we used Wolfs method [31] to calculate the finite time LEs for a period of 25000s.

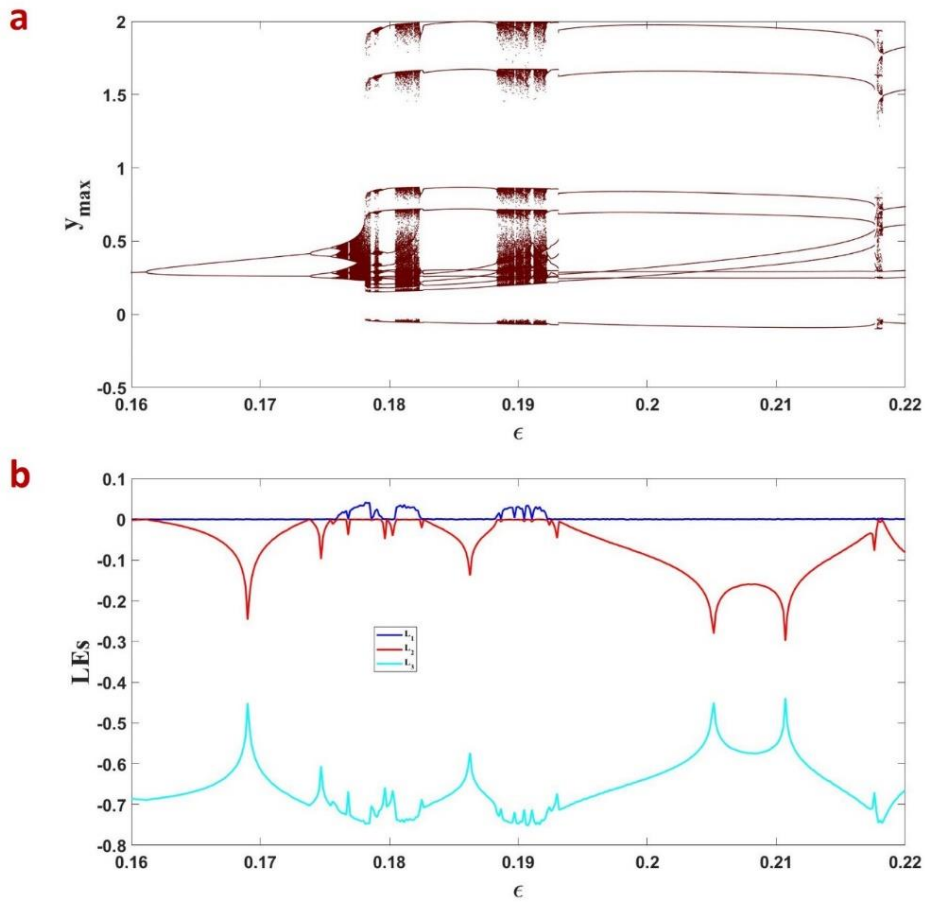


Fig.4:a) Bifurcation of the system (3) with  $\epsilon$ ; b) Corresponding LEs

To understand the multistability behaviors of the system, we derive the bifurcation transition diagrams using forward (increasing the parameter and plotting the local maxima of the state

variable with reinitializing the initial conditions) and backward (decreasing the parameter and plotting the local maxima of the state variable with reinitializing the initial conditions) iterations. This is shown in the Fig.5 where forward continuation is shown in blue and backward in red.

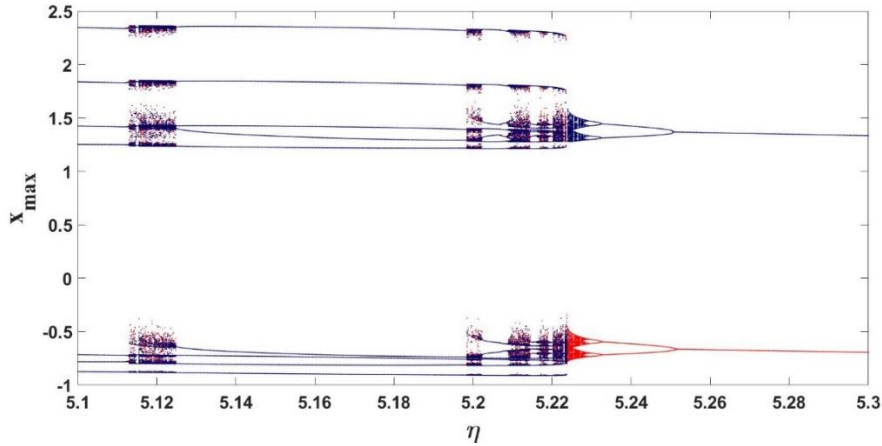


Fig.5: Bifurcation of the system (3) with  $\eta$  for forward (blue) and backward (red) continuation

It is to be noted that we have used RK4 method for the numerical simulation of the Pernarowski model and to derive the forward and backward continuation we used reinitialising of the initial conditions to the end values of the state trajectories in every iteration and decrease or increase the parameter.

#### 4. Spiral waves in Pernarowski model

The investigation of wave propagation phenomenon in Pernarowski model of pancreatic  $\beta$  cells is of interest as this has not been investigated in the literatures. To remedy this omission, we constructed a  $110 \times 110$  network of  $\beta$  cells and local dynamics of the cells in the network are governed by the system shown in (21) and in order to generate plane waves in the network, we imposed an external stimuli ( $A \cos(\omega t)$ ) to the left boundary of the network. The primary motive of applying plane waves to the left boundary is to capture the existing spiral waves in the network as the plane waves move from left to right boundary. We used the Runge-Kutta 4<sup>th</sup> order for the numerical analysis of the network with the initial states of the variables are  $(x, y, z) = (0, 0, 0)$ . We considered  $b = 0$  for deriving Fig.6 to Fig.8.

The  $\beta$  cells network of  $110 \times 110$  cells can be defined as,

$$\begin{aligned} \dot{x}_{ij} &= y_{ij} + D(V_{i+1j} + V_{i-1j} + V_{ij+1} + V_{ij-1} - 4V_{ij}) + \psi(t)\zeta_{i\theta_1}\zeta_{j\theta_2} \\ \dot{y}_{ij} &= -(a((x_{ij} - b)^2 - \eta^2))y_{ij} - (z_{ij} + x_{ij}^3 - 3(x_{ij} + 1)) - \varepsilon(\beta(x_{ij} - c) - z_{ij}) \\ \dot{z} &= \varepsilon(\beta(x_{ij} - c) - z_{ij}) \end{aligned} \quad (21)$$

where  $\psi(t) = A \cos(\omega t)$  is the induced force and  $\zeta_{i\theta_1} = 1, \zeta_{j\theta_2} = 1$  exists for  $i = \theta_1, j = \theta_2$  respectively. We have investigated the plane wave propagation in the network by considering

different amplitudes and frequencies of the induced force, different values of the system parameters and different coupling strengths.

A minimum size of the domain, necessary to support the occurrence of a spiral wave [39]. The said size of the network could reliably simulate the development of a spiral wave. We investigate the patterns of the waves that are formed by applying different  $\psi(t)$  and external periodical force on the main diameter of the plane with different values of  $A$  and  $\omega$ . For the numerical simulation of the network, we have used the RK4 method with a step size of 0.01.

#### 4.1 Different values of induced force frequency ( $\omega$ ):

In this subsection we discuss the effect of the frequency of the induced force on the spiral wave formation in the network. For this discussion we consider the case  $b = 0$  with the coupling coefficient  $D = 0.5$  and the other system parameters as in (5). The stimuli amplitude is kept as  $A = 0.01$ . Fig.6 shows the spatiotemporal snapshots taken at 5000 time units. We observe the spiral waves even for a low stimuli frequency of 0.0001 and the spiral waves are destroyed by the travelling plane waves when the frequency is increased to  $\omega = 3$ . The spiral waves keeps seperating as the spiral seeds multiply with increase in frequency till  $\omega = 0.5$ . After this the spiral seeds combine and gets destroyed for higher frequencies as seen in Fig.6. Thus by increasing the plane wave frequency we can destroy the spiral waves created in the network.

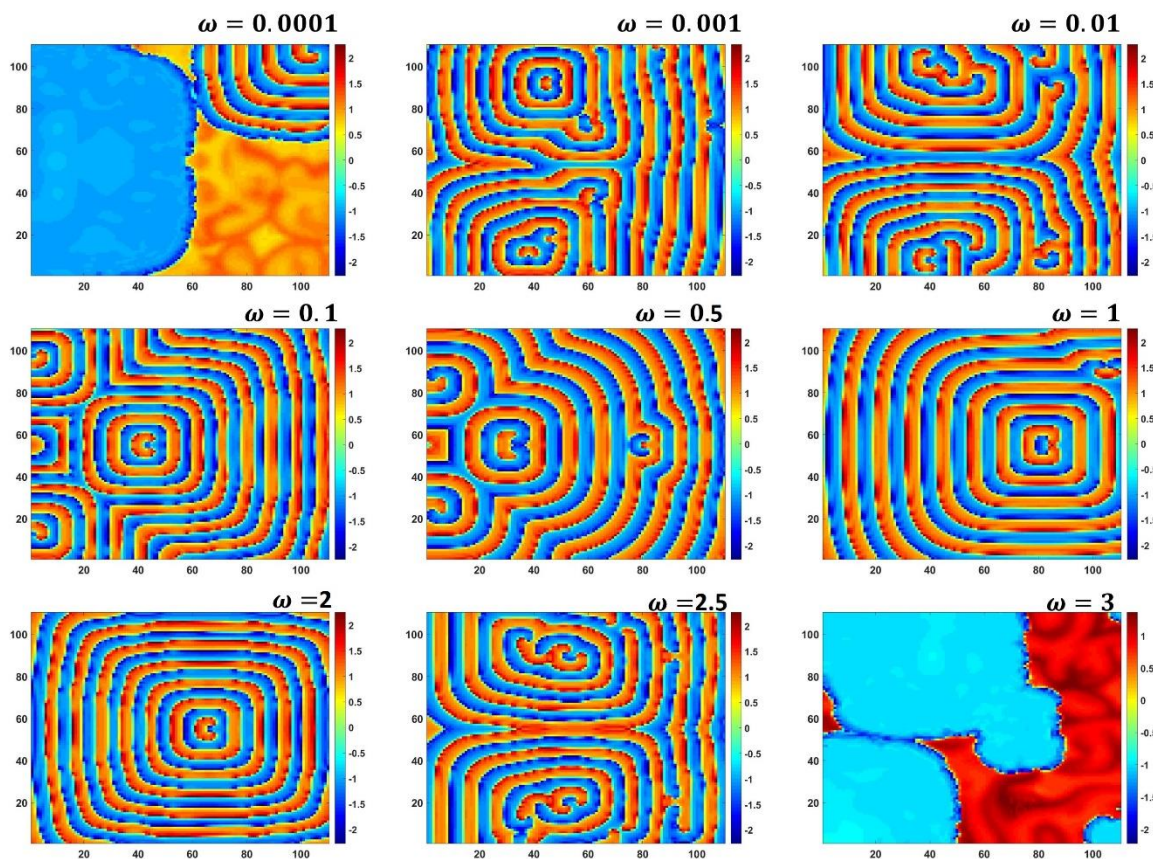


Fig.6: Spatiotemporal snapshot of the network (21) for  $D = 0.5, A = 0.01$  and various induced force frequencies. The other system parameters are  $a = -0.02, \beta = 2, c = -1.5, \eta = 5.224, \varepsilon = 0.178$

#### 4.2 Different values of induced force amplitude ( $A$ ):

In Fig.6 we show that by increasing the stimuli frequency the spiral waves can be destroyed. In this subsection we show the effect of stimuli amplitude on the spiral waves in the network. We fix the frequency of the stimuli wave as  $\omega = 0.01$  and coupling coefficient as  $D = 0.5$ . The other system parameters are as in (5) and we show the snapshots of the network at 5000 time units as shown in Fig.7. For lower amplitudes the spiral waves are not disturbed by the plane waves but by increasing the amplitude to 0.1 the travelling plane waves destroy the spiral waves in the network. Hence again the plane wave components (amplitude and frequency) can be properly tuned to destroy the spiral waves in the network.

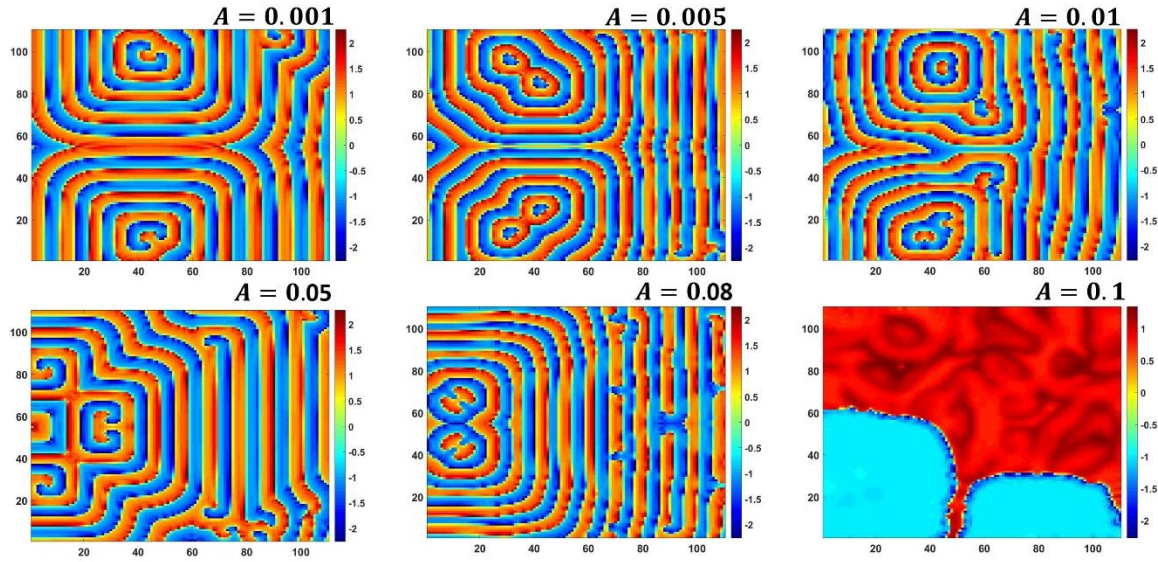


Fig.7: Spatiotemporal snapshot of the network (21) for  $D = 0.5$ ,  $\omega = 0.001$  and various induced force amplitudes. The other system parameters are  $a = -0.02$ ,  $\beta = 2$ ,  $c = -1.5$ ,  $\eta = 5.224$ ,  $\varepsilon = 0.178$

#### 4.3 Different values of coupling coefficient ( $D$ ):

As we know that the coupling coefficient or the coupling strength between the neighboring neurons play an important role in the generation of spiral waves, we investigate the effect of the coupling coefficient on the spiral waves. We choose various coupling strengths and fix the plane wave amplitude and frequency as  $A = 0.01$ ,  $\omega = 0.01$  and present the spatiotemporal snapshots of the network in Fig.8. We see that only for  $D = 0.4$  and  $D = 0.5$  could the spiral waves be generated by the network. Normally for higher coupling strengths close to '1' spiral waves can be seen in many of the neuron networks but not in this case; even for  $D = 0.55$  the network dissipates the spiral waves and the plane waves can be seen travelling through the network.



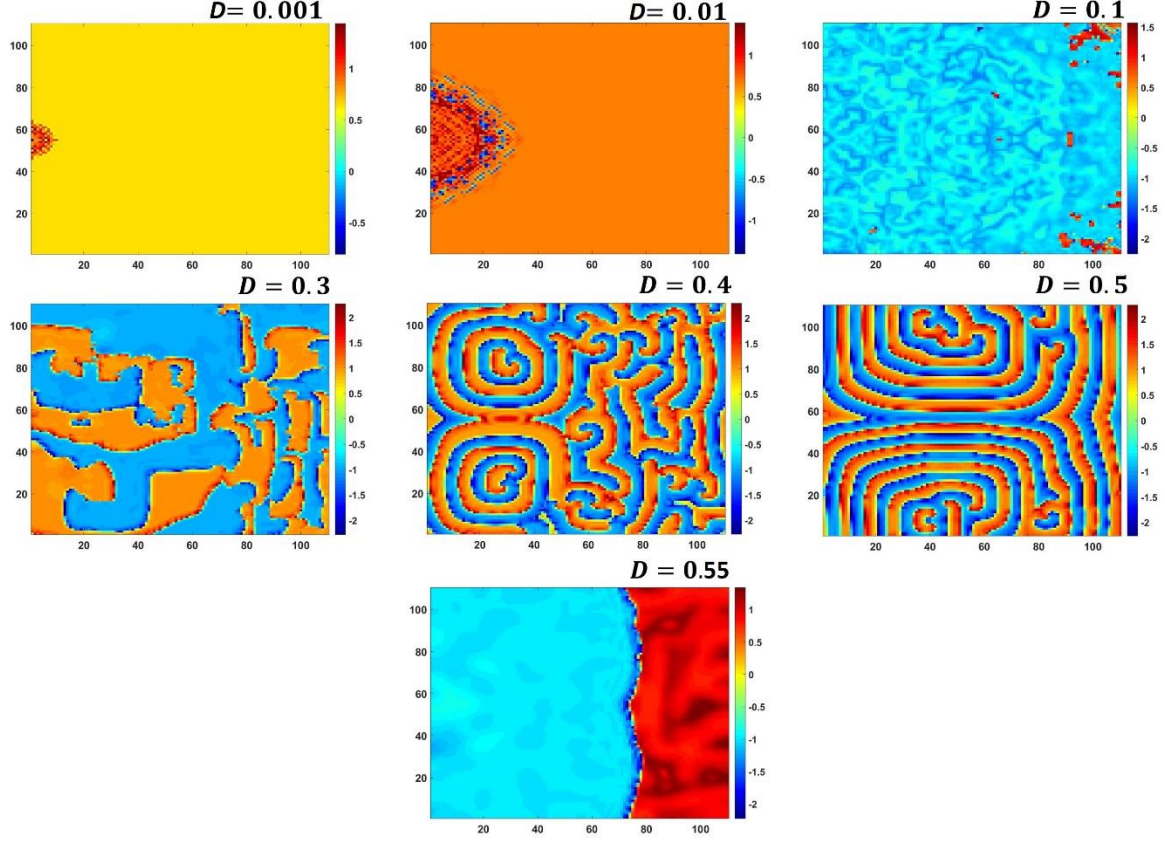


Fig.8: Spatiotemporal snapshot of the network (21) for  $\omega = 0.01, A = 0.01$  and various values of the coupling coefficient  $D$ . The other system parameters are  $a = -0.02, \beta = 2, c = -1.5, \eta = 5.224, \varepsilon = 0.178$

#### 4.4 Different values of parameter $b$ :

After discussing the stimuli force and the coupling coefficient effect on the spiral wave in the network, our interest is now on the investigation of individual  $\beta$  cell effect on the spiral wave generation. For this we consider the parameter  $b$  as the control variable while keeping the stimuli parameters as  $A = 0.01, \omega = 0.01$ , coupling coefficient  $D = 0.5$  and the other system parameters as in (5). The spiral waves are seen in the network as long as  $b = 0.08$  as after this value the plane wave amplitudes are much higher than the limit cycle amplitude of the cells and hence the spiral waves are easily destroyed by the plane waves. We have shown the spatiotemporal snapshots in Fig.9.

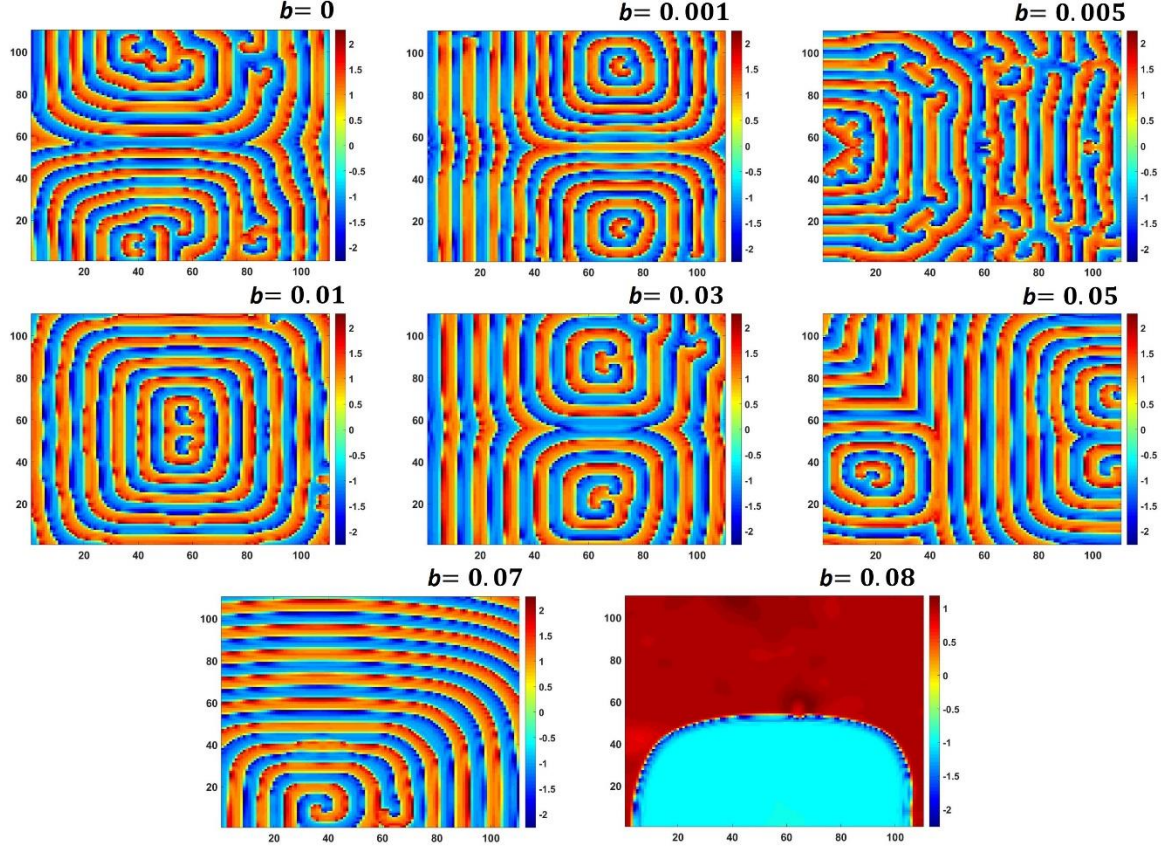


Fig.9: Spatiotemporal snapshot of the network (21) for  $D = 0.5$ ,  $\omega = 0.01$ ,  $A = 0.01$  and various values of  $b$ . The other system parameters are  $a = -0.02$ ,  $\beta = 2$ ,  $c = -1.5$ ,  $\varepsilon = 0.178$ ,  $\eta = 5.224$

### 5. Spiral waves in a two layer Pernarowski beta cell network

To investigate the spatiotemporal dynamics of the two-layer Pernarowski network, we have constructed the network using two separate lattices of betacells coupled as shown in Equation (22). In each of the layer we have  $100 \times 100$  neurons whose local dynamics is governed by the Pernarowski beta cell model. We have considered a periodic stimulus  $A \sin(\omega t)$  and the spatiotemporal behavior of the two-layer network is investigated as discussed below.

$$\begin{aligned}
\text{Layer-1} & \begin{cases} \dot{x}_{1,ij} = (y_{1,ij}) + D_{1,1}(x_{1,i+1j} + x_{1,i-1j} + x_{1,ij+1} + x_{1,ij-1} - 4x_{1,ij}) \\ \quad + D_2(x_{2,ij} - x_{1,ij}) + \psi(t)\zeta_{i\theta_1}\zeta_{j\theta_2} \\ \dot{y}_{1,ij} = -(a((x_{1,ij} - b)^2 - \eta^2))y_{1,ij} - (z_{1,ij} + x_{1,ij}^3 - 3(x_{1,ij} + 1)) \\ \quad - \varepsilon(\beta(x_{1,ij} - c) - z_{1,ij}) \\ \dot{z}_{1,ij} = \varepsilon(\beta(x_{1,ij} - c) - z_{1,ij}) \end{cases} \\
\text{Layer-2} & \begin{cases} \dot{x}_{2,ij} = (y_{2,ij}) + D_{2,2}(x_{2,i+1j} + x_{2,i-1j} + x_{2,ij+1} + x_{2,ij-1} - 4x_{2,ij}) \\ \quad + D_2(x_{1,ij} - x_{2,ij}) + \psi(t)\zeta_{i\theta_1}\zeta_{j\theta_2} \\ \dot{y}_{2,ij} = -(a((x_{2,ij} - b)^2 - \eta^2))y_{2,ij} - (z_{2,ij} + x_{2,ij}^3 - 3(x_{2,ij} + 1)) \\ \quad - \varepsilon(\beta(x_{2,ij} - c) - z_{2,ij}) \\ \dot{z}_{2,ij} = \varepsilon(\beta(x_{2,ij} - c) - z_{2,ij}) \end{cases}
\end{aligned} \tag{22}$$

The subscript  $(K, ij)$  in (22) represents layer- $K$  ( $K \in (1,2)$ ) lattice network with  $(ij)$  showing the location of the beta cell in the network.  $D_{1,1}, D_{2,2}$  represents the coupling strength of the neurons in the respective layers of the lattice network and  $D_2$  represents the inter layer coupling strength between layer-1 and layer-2. When  $\zeta_{i\theta_1} = \zeta_{j\theta_2} = 1$  when  $\theta_1 = i, \theta_2 = j$ , the stimuli force is applied to the network and in our case we choose  $\theta_1 = 1:100, \theta_2 = 1$  such that the stimuli is applied to the left boundary of the network.

The snapshots are shown for 1000 time-units and the initial condition of the neurons in Layer-1 is  $[0,0,0]$ , whereas the initial condition of Layer-2 is  $[0,0,0]$  except for the neurons in the following locations:

$$x(30:70,48:50) = 0.02; x(30:70,51:53) = 0.05; x(30:70,54:56) = 0.01;$$

$$y(30:70,48:50) = 0.01; y(30:70,51:53) = 0.01; y(30:70,54:56) = 0.01;$$

$$z(30:70,48:50) = 0.01; z(30:70,51:53) = 0.03; z(30:70,54:56) = 0.05;$$

We have adopted this initial condition setup from [34] as it was proved that such initial condition setup will initiate spiral waves in both layers. In the discussions below, we will be showing the effect of the inter layer coupling ( $D_2$ ) and the stimuli amplitude ( $A$ ). The readers are encouraged to try the effect of the stimuli amplitude and also the parameter effects on the spiral waves in the Two-layer network.

### 5.1 Effect of the inter layer coupling

In this section we will study the effect of the inter layer coupling ( $D_2$ ) on the spiral wave generation in both the layers of the Two-layer network. For this simulation we consider commensurate intra layer coupling ( $D_{1,1} = D_{2,2} = 0.5$ ), the parameters as in (5) and the stimuli amplitude  $A = 0.5$  and stimuli frequency  $\omega = 0.05$ . In Fig.10 we have kept the intra layer coupling as 0.01 and simulated the network. The spatio temporal dynamics are captured at four different time intervals at  $T=100,300,600,1000$ . As the stimuli force enters the network at the left boundary, we could see that both the layers doesn't show any spiral waves and thus the

applied stimuli doesn't affect the dynamics of the network and couldn't capture the spiral turbulence.

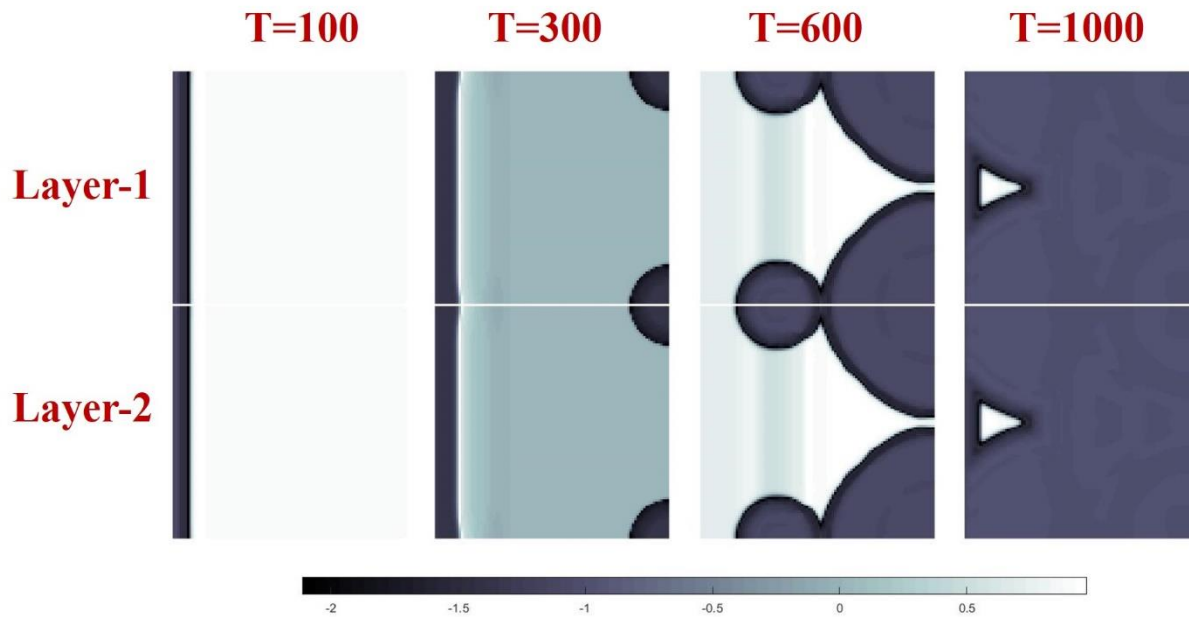


Fig.10: Spatiotemporal dynamics of the two layer beta cell network with the intra layer coupling  $D_2 = 0.01$ . The snapshots are taken at four different time intervals (in secs) as shown in the figure. Layer-1 denotes the upper layer and layer-2 denotes the lower layer.

As the inter layer coupling at 0.01 doesn't show any signs of the spiral waves, we now increase the coupling strength to 0.03 and we capture the spatiotemporal dynamics as shown in Fig.11. Now at the initial phase ( $T < 200$ ), the stimuli force just pass the network as just simple travelling waves. But at time  $T=300$ , the spiral seeds are generated simultaneously in both the layers as in Fig.11 and further develops in to a complete spiral turbulence in both the layers. It should be noted that the spiral seeds are symmetric and the seeds originate from the topleft and bottom left corners of the network. Also we could see that both the layers are in perfect synchrony even for a smallest coupling of 0.03.



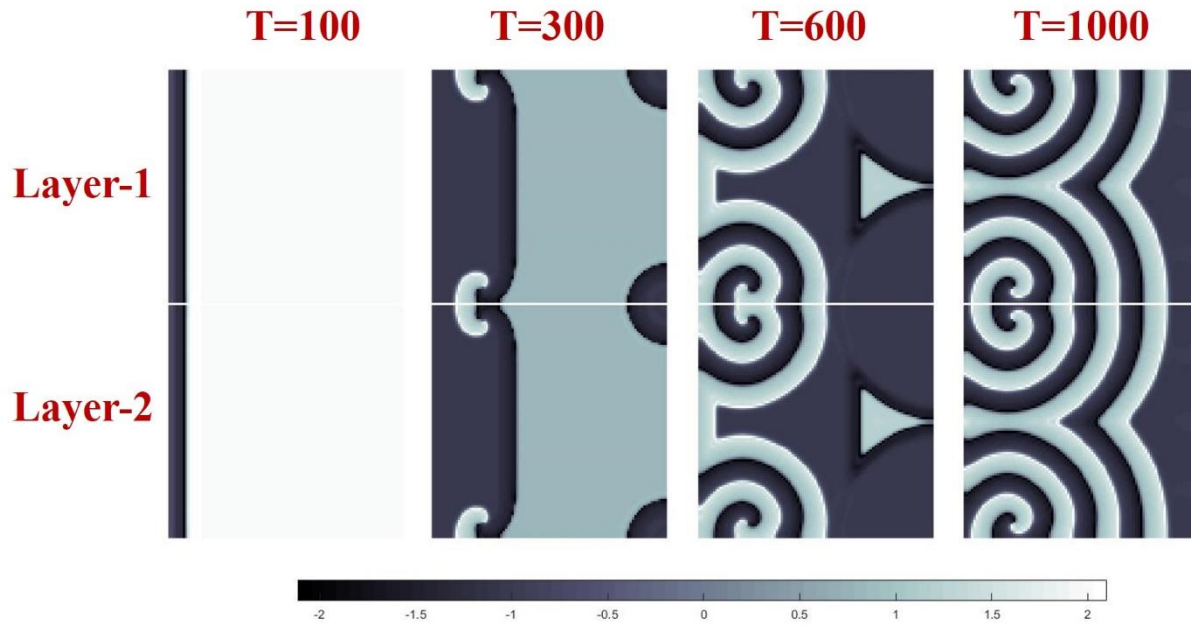


Fig.11: Spatiotemporal dynamics of the two layer beta cell network with the intra layer coupling  $D_2 = 0.03$ . The snapshots are taken at four different time intervals (in secs) as shown in the figure. Layer-1 denotes the upper layer and layer-2 denotes the lower layer.

Further increasing the inter layer coupling to 0.05, we could see the complete elimination of the spiral waves in the network. From this we could conclude that for  $0.023 < D < 0.034$ , the spiral waves are seen in both the layers and hence inter layer coupling can play an important role in the existence of spiral turbulence in the network.

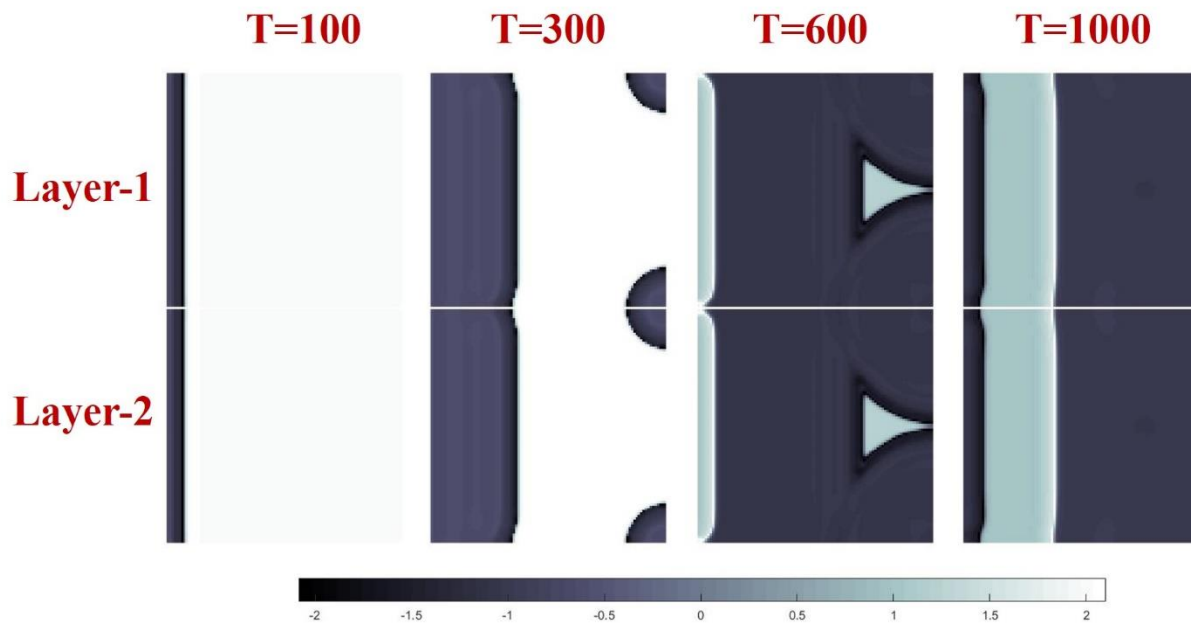


Fig.12: Spatiotemporal dynamics of the two layer beta cell network with the intra layer coupling  $D_2 = 0.01$ . The snapshots are taken at four different time intervals (in secs) as shown in the figure. Layer-1 denotes the upper layer and layer-2 denotes the lower layer.

### 5.2 Effect of the stimuli amplitude

Investigating the effect of the applied force on the network is of interest in order to see the controlling of the spiral turbulence. Hence we now discuss the effect of the stimuli amplitude  $A$  on the spiral wave existence. For this simulation we consider commensurate intra layer coupling ( $D_{1,1} = D_{2,2} = 0.5$ ), the inter layer coupling  $D_2 = 0.03$ , the parameters as in (5) and stimuli frequency  $\omega = 0.05$ . To start with, we choose a lower amplitude of  $A = 0.1$  and we captured the spatiotemporal behavior of both the layers as shown in Fig.13. For the initial time periods of  $T < 250s$  there is no spiral wave seeds seen in the network. But after  $T > 250s$ , the spiral seeds are captured in the network originating at the left boundary. As the frequency is kept at 0.05, the spiral turbulence travel smoothly through the network and expands out as larger plane waves when they reach the right boundary. Again we could see that both the layers are in perfect synchrony and exhibits similar patterns of spiral waves.

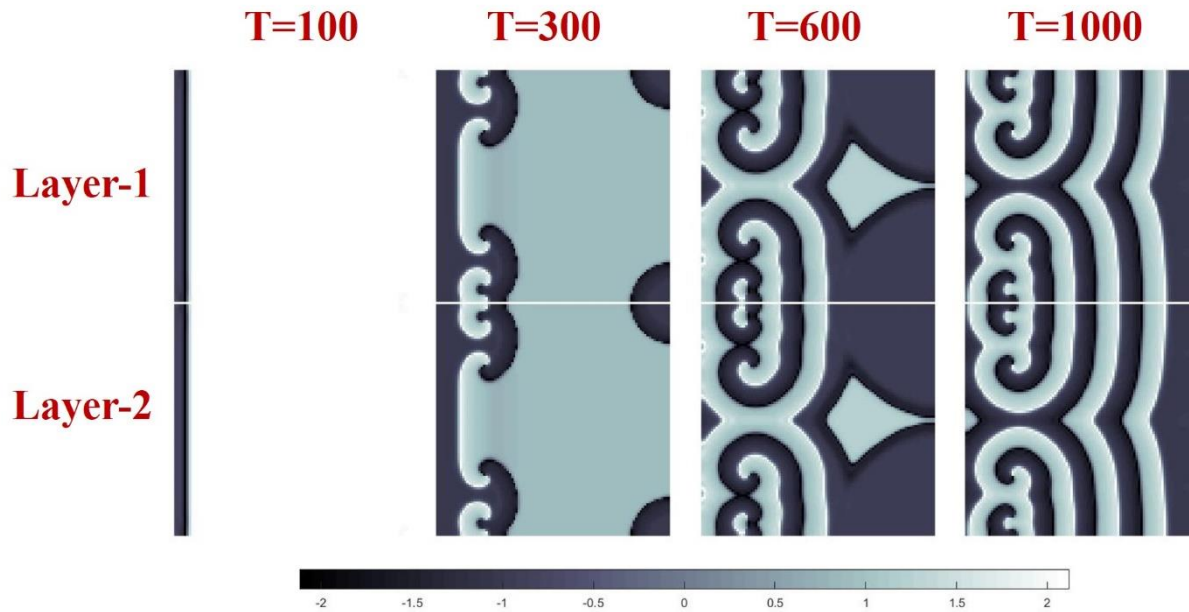


Fig.13: Spatiotemporal dynamics of the two layer beta cell network with the stimuli amplitude  $A=0.1$  while keeping the stimuli frequency at  $\omega = 0.05$ . The snapshots are taken at four different time intervals (in secs) as shown in the figure. Layer-1 denotes the upper layer and layer-2 denotes the lower layer.

Now by increasing the stimuli amplitude to  $A=0.3$ , we could notice the termination of spiral waves as in Fig.14. This shows that by controlling the stimuli amplitude, we could control the spiralwave turbulence in the network. The plane waves entering at very low frequency at the left boundary exits the network with no spiral seeds seen in the network. We could also confirm

that there do not exist spiral waves even by increasing the frequency further till 0.5. This proves that we can suppress the spiral turbulence by proper selection of the periodic stimuli.

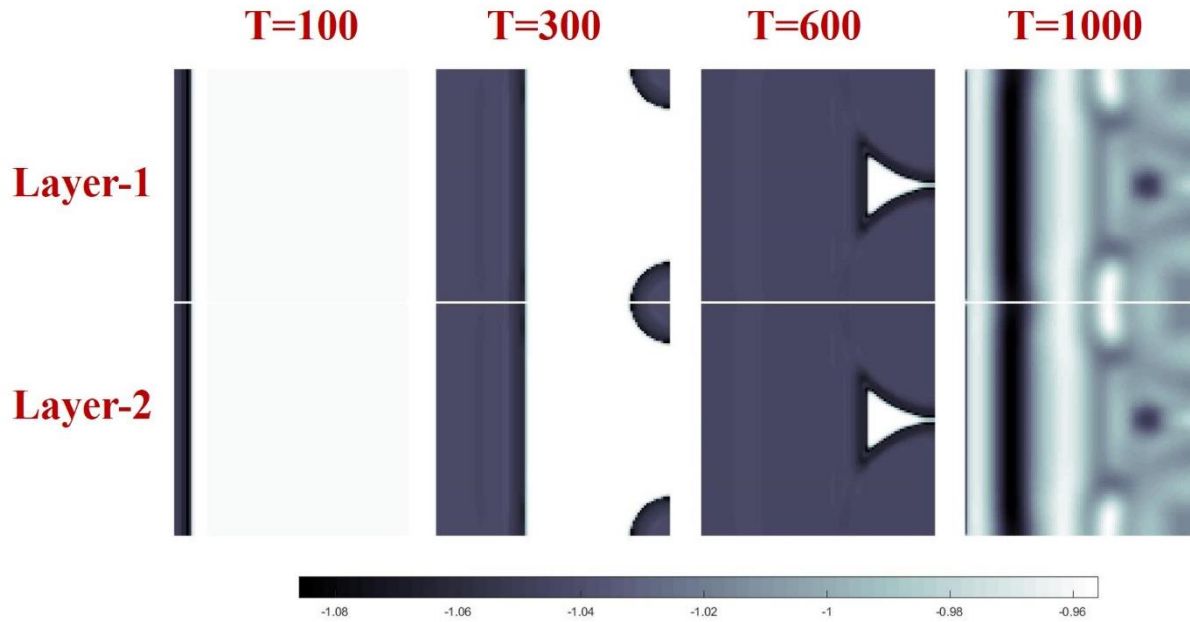


Fig.14: Spatiotemporal dynamics of the two layer beta cell network with the stimuli amplitude  $A=0.3$  while keeping the stimuli frequency at  $\omega = 0.05$ . The snapshots are taken at four different time intervals (in secs) as shown in the figure. Layer-1 denotes the upper layer and layer-2 denotes the lower layer.

As seen in Fig.14, we showed that for  $A=0.3$ , the spiral waves are terminated. Most of the literatures agree that once a spiral wave is terminated in the network by either an amplitude or a frequency of the stimuli, we may take that the spiral waves may not emerge again in the network when we increase the stimuli parameter. But this was not the case in this network as when we increase the amplitude to  $A=0.5$ , the spiral waves reappear in the network which is much stronger than that in Fig.13 which can be seen in Fig.15. Thus this network exhibits spiral waves in two different amplitude ranges and for suppressing these waves we have to be accurate enough in selecting the stimuli amplitude. We have further increased the amplitude but there is no spiral waves seen in the network.

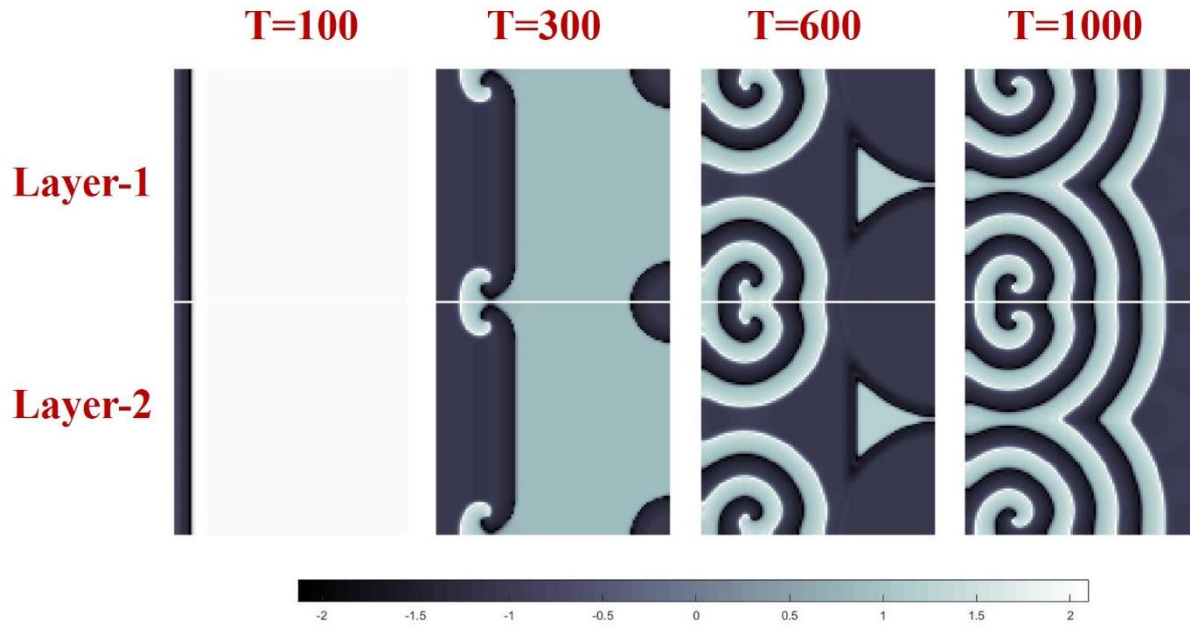


Fig.15: Spatiotemporal dynamics of the two layer beta cell network with the stimuli amplitude  $A=0.5$  while keeping the stimuli frequency at  $\omega = 0.05$ . The snapshots are taken at four different time intervals (in secs) as shown in the figure. Layer-1 denotes the upper layer and layer-2 denotes the lower layer.

A coordinated functioning of beta cell clusters within pancreatic islets is governed through gap junction [40-42]. It is arbitrated by oscillatory membrane depolarization and consequent changes in cytoplasmic calcium concentration. Such clusters, called the islets of Langerhans. When gap junctions permit for intraislet information exchange, islets containing beta cells formulate complex syncytia which is complex nonlinear and highly heterogeneous [41-43]. Horde of Literatures [44-46] highlighted the possibility of wave-like activity in the islets. It is worth noting  $\text{Ca}^{2+}$  signals are not likely to propagate through non- $\beta$ -cells in the islets of Langerhans. The spatiotemporal  $\text{Ca}^{+}$  dynamics within these syncytia is studied with the influence of intercellular coupling term[47-49]. In particular, the first few minutes after stimulation, the probability distribution of calcium wave is characterized with critical behaviour. Variations in induced force terms and coupling coefficients, the dynamics changes qualitatively such that the number of global intercellular calcium events increases to the point where the behaviour becomes supercritical. Our results reveal that the variation of oscillatory changes, along with rise in plasma glucose observed in diabetes, could be associated with a switch to supercritical calcium dynamics and loss of beta cell functionality. After raising the glucose level, all the cells need not start the bursting activity and insulin secretion at the same time.

In summary, more than one mechanism for wave propagation in the islets of Langerhans exists. A variety of such mechanisms shows only that waves in the islets of Langerhans are not rare and needs to be accounted for to understand the coordination mechanisms in the islets. Glucose is the most important initiator of the bursting activity in the islets of Langerhans; hence the study on influence of the wave propagation regimes is vital. Thus, the possible physiological

role of waves in the living islets is clear: at the initial stages of the  $\beta$ -cell response to glucose stimulation, such waves can provide an optimal way for transmission of electrical/calcium signals for insulin secretion from the bursting cells to the silent ones, initiating the secretion process in regions with less glucose and not yet active.

## Conclusion

In this paper we have discussed the Pernarowski model of pancreatic  $\beta$  cells and have derived the various dynamical properties of the model. The chaotic spiking and periodic bursting regions of the model are discussed using the bifurcation plots. To investigate the network dynamics, we constructed One-layer and Two-layer network of  $\beta$  cells and an external stimulus is applied to the network. In a One-layer network we have shown that by properly changing the frequency and amplitude of the stimuli we showed that we can suppress spiral waves in the network.

In many literatures it is shown that the effect of neural coupling strength affects the timely pattern of neural synchronization and significantly changes when the neurons are allowed to more communicate with one another. In fact, very weak coupling between the neurons resulted in tiny or no spirals. But in this paper we have shown that when the coupling strength is increased, the spiral waves disappear confirming that neuron communication and their synchronization with lesser coupling can also generate spiral waves. This can be checked in both One-layer and Two-layer networks wherein we kept the coupling strength as  $D=0.5$  in One-layer network and  $D_{1,1} = D_{2,2} = 0.5$  in a Two-layer network.

For further investigation, we also performed the amplitude examinations in both one-layer and two-layer network. Our results revealed that, in a both types of neural network, by properly adjusting the amplitude and frequency (one-layer) or amplitude (two-layer) of the electrical stimuli, both of these factors could help to control or even eliminate the spiral waves.

## References

- [1]. Weir GC, Bonner-Weir S, "Islet beta cell mass in diabetes and how it relates to function, birth, and death". Ann N Y Acad Sci. 2013; 1281:92–105. [PubMed: 23363033], (2013)
- [2]. P. Gilon, M. A. Ravier, J.-C. Jonas, and J.-C. Henquin, "control mechanism of the oscillation of insulin secretion in vitro and in vivo", Diabetes 51(1), S144-S151, (2002).
- [3]. R. Bertram, A. Sherman, and L. S. Satin, "Metabolic and electrical oscillations: partners in controlling pulsatile insulin secretion", Am. J. Physiol. Endocrinol. Metab. 293, E890 (2007).
- [4]. P. Rorsman, M. Braun, "Regulation of insulin secretion in human pancreatic islets" Annu. Rev. Physiol. 75, 155-179, (2013).
- [5]. N. Pørksen, "The in vivo regulation of pulsatile insulin secretion" Diabetologia 45, 3 (2002).
- [6]. L. S. Satin, P. C. Butler, J. Ha, and A. S. Sherman, "Pulsatile Insulin Secretion, Impaired Glucose Tolerance and Type 2 diabetes", Mol. Aspects Med. 42, 61-77, (2015).
- [7]. Richard Bertram, Arthur Sherman, "Dynamical complexity and temporal plasticity in pancreatic b-cells", J. Biosci., vol. 25, No. 2, (2000).

- [8]. H. Fallah, "Chaos in Parnarowski model of Panccreatic beta-cells", Proceedings of the 47<sup>th</sup> Annual Iranian Mathematics conference. Pages: 956-960, (2016).
- [9]. Jorge Duarte, Cristina Januario, Nuno Martins, "A Chaotic Bursting-Spiking transition in a Pancreatic Beta-Cells System: Observation of an interior Glucose-Induced crisis", Mathematical Biosciences And Engineering 14 (4), 821-842 (2017), , Doi:10.3934/mbe.2017045
- [10]. Gerda De Vriesy, Robert M. Miura, "Analysis of a class of models of bursting electrical Activity in pancreatic Beta-cells", SIAM J. APPL. MATH, Society for Industrial and Applied Mathematics, 58, (2), 607-635, (1998).
- [11]. J.M.W. van de Weem, J.G. Barajas Ram'irez, R. Femat, H. Nijmeijer, "Conditions for synchronization and chaos in networks of  $\beta$ -cells", 2<sup>nd</sup> IFAC Conference on Analysis and Control of Chaotic Systems, 42 (7), 176-181, (2009). DOI: 10.3182/20090622-3-UK-3004.00035
- [12]. Ma Xindong, Cao Shuqian, Guo Hulun, "Routes to bursting oscillations in a modified van der Pol–Duffing oscillator with slow-varying periodic excitation", Journal of Vibration and Control 0(0), 1-11, SAGE Publications, (2017). DOI: 10.1177/1077546317740020
- [13]. Alessandro Loppini and Morten Gram Pedersen, "Gap-junction coupling can prolong beta-cell burst period by an order of magnitude via phantom bursting", CHAOS 28, 063111 (2018).
- [14]. G. de Vries, "Multiple Bifurcations in a Polynomial Model of Bursting Oscillations", J. Nonlinear Sci. Vol. 8: 281–316, (1998).
- [15]. Eugene M. Izhikevich, "Neural Excitability, Spiking And Bursting", International Journal of Bifurcation and Chaos, Vol. 10, No. 6, 1171-1266, (2000).
- [16]. M. Parnarowski, "Fast and Slow Subsystems for a continuum model of bursting activity in the Pancreatic Islet", SIAM Journal on Applied Mathematics 58(5), (1998). DOI: 10.1137/S0036139996304585
- [17]. Iulia Martina Bulai, Morten Gram Pedersen, "Stopping waves: geometric analysis of coupled bursters in an asymmetric excitation field", Nonlinear Dyn, Springer Nature B.V. (2019). DOI:10.1007/s11071-019-04895-w
- [18]. Karthikeyan Rajagopal , Fatemeh Parastesh, Hamed Azarnoush, Boshra Hatef , Sajad Jafari , Vesna Berec, "Spiral waves in externally excited neuronal network: Solvable model with a monotonically differentiable magnetic flux", Chaos 29, 043109, (2019). DOI:10.1063/1.5088654
- [19]. Rinzel J, "A formal classification of bursting mechanisms in excitable systems.; in Lecture notes in biomathematics: mathematical topics in population biology, morphogenesis, and neurosciences (eds) E Teramoto and M Yamaguti (New York: Springer-Verlag) vol. 71, 267–281, (1987).
- [20]. R. Fitzhugh, Impulses and physiological states in theoretical models of nerve membrane, Biophys. J., 1 , 445–466. (1961).
- [21]. V. K. Mel'nikov, "On the stability of the center for time-periodic perturbations", Trans. Moscow, Math. Soc., 12 (1963), pp. 1-57. (1963).
- [22]. Pedersen, M., Bertram, R., and Sherman, A, "Intraand inter-islet synchroization of metabolically driven insulin secretion. Biophysical journal, 89, 107–119, (2005).
- [23]. Chay, T. R. "Glucose response to bursting-spiking pancreatic beta-cells by a barrier kinetic model," Biol.Cybern. 52, 339–349, (1985).



- [24]. M. Pernarowski, “Fast subsystem bifurcations in a slowly varying Liénard system exhibiting bursting”, *SIAM J. Appl. Math.*, 54, 814–832. (1994)
- [25]. Haniyeh Fallah, “Symmetric Fold/Super-Hopf Bursting, Chaos and Mixed-Mode Oscillations in Pernarowski Model of Pancreatic Beta-Cells”, *International Journal of Bifurcation and Chaos*, . 26, (9) (2016).
- [26]. Kuznetsov, Y. A. “Elements of Applied Bifurcation Theory”, Springer-Verlag, NY, (2004).
- [27]. Mello, L. F, Coelho, S. F. “Degenerate Hopf bifurcations in the  $L\ddot{u}$  system”, *Phys. Lett. A* 2009, 373: 1116-1120. (2009)
- [28]. Sotomayor, S., Mello, L. F Braga, D. C. “Bifurcation analysis of the Watt governor system, *Comm. Appl. Math.* 2007, 26: 19-44. (2007)
- [29]. Sotomayor, S., Mello, L. F. & Braga, D. C.” Lyapunov coefficients for degenerate Hopf bifurcations”, (2007), arXiv:0709.3949v1 [math.DS],
- [30]. Zhouchao Wei, Yingying Li, Bo Sang, Yongjian Liu, Wei Zhang. “Complex dynamical behaviors in a 3D simple chaotic flow with 3D stable or 3D unstable manifolds of a single equilibrium”, *International Journal of Bifurcation and Chaos* 29(7), 1950095, (2019).
- [31]. A. Wolf, J. B. Swift, H. L. Swinney, J. A. Vastano, "Determining Lyapunov exponents from a time series," *Physica D: Nonlinear Phenomena*, . 16, 285-317, (1985).
- [32]. M. Lv, J. Ma, Y. Yao, and F. Alzahrani, “Synchronization and wave propagation in neuronal network under field coupling,” *Sci. China Technol. Sci.* 62, 1–10, (2018).
- [33]. B. Hu, J. Ma, and J. Tang, “Selection of multiarmed spiral waves in a regular network of neurons,” *PLoS One* 8, e69251, (2013).
- [34]. Peraza, L.R., et al., “Electroencephalographic derived network differences in Lewy body dementia compared to Alzheimer’s disease patients”. *Scientific reports*, **8**(1), 4637. (2018).
- [35]. D.Baleanu, A. Jajarmi, S.S.Sajjadi, J.H.Asad, “The fractional features of a harmonic oscillator with position-dependent mass”, *Communications in Theoretical Physics* 72 (5), 055002, (2020).
- [36]. A. Jajarmi, A. Yusuf, D.Baleanu, M. Inc, “A new fractional HRSV model and its optimal control: A non-singular operator approach”, *Physica A: Statistical Mechanics and its Applications* 547, 123860, (2020).
- [37]. D.Baleanu, A. Jajarmi, H. Mohammadi, S.Rezapour, “A new study on the mathematical modelling of human liver with Caputo-Fabrizio fractional derivative”, *Chaos, Solitons & Fractals* 134, 109705, (2020).
- [38]. A. Jajarmi, D.Baleanu, S.S.Sajjadi, J.H.Asad, “A new feature of the fractional Euler-Lagrange equations for a coupled oscillator using a nonsingular operator approach”, *Frontiers in Physics* 7, 196, (2019).
- [39]. J. Yang, M. Zhang, “The investigation of the minimum size of the domain supporting a spiral wave in oscillatory media”, *Phys Lett A*, 352: 69–72 (2006).
- [40]. Benninger, R. K. P., Zhang, M., Head, W. S., Satin, L. S., and Piston, D. W. “Gap junction coupling and calcium waves in the pancreatic islet”, *Biophys. J.* 95, 5048–5061. (2008).

- [41]. Benninger, R. K. P. P., Hutchens, T., Head, W. S., McCaughey, M. J., Zhang, M., Le Marchand, S. J., et al. “Intrinsic islet heterogeneity and gap junction coupling determine spatiotemporal Ca<sup>2+</sup> wave dynamics”. *Biophys. J.* 107, 2723–2733. (2014).
- [42]. Cappon, G., and Pedersen, M. G. “Heterogeneity and nearest-neighbor coupling can explain small-worldness and wave properties in pancreatic islets”, *Chaos* 26, 53103–53107. (2016).
- [43]. Charollais, A., Gjinovci, A., Huarte, J., Bauquis, J., Nadal, A., Martín, F., et al. “Junctional communication of pancreatic  $\beta$  cells contributes to the control of insulin secretion and glucose tolerance”, *J. Clin. Invest.* 106, 235–243. (2000).
- [44]. Cherubini, C., Filippi, S., Gizzi, A., and Loppini, A. “Role of topology in complex functional networks of beta cells”, *Phys. Rev. E* 92, 42702–42712. (2015).
- [45]. Dolenšek, J., Stožer, A., Skelin Klemen, M., Miller, E. W., and Slak Rupnik, M. The relationship between membrane potential and calcium dynamics in glucose-stimulated beta cell syncytium in acute mouse pancreas tissue slices. *PLoS ONE* 8:e82374. (2013).
- [46]. Eddlestone, G. T., Gonçalves, A., Bingham, J. A., and Rojas, E. Electrical coupling between cells in islets of Langerhans from mouse. *J. Membr. Biol.* 77, 1–14. (1984).
- [47]. Gosak, M., Dolenšek, J., Markovič, R., Slak Rupnik, M., Marhl, M., and Stožer, A. Multilayer network representation of membrane potential and cytosolic calcium concentration dynamics in beta cells. *Chaos Solitons Fractals* 80, 76–82. (2015).
- [48]. Gosak, M., Markovič, R., Dolenšek, J., Slak Rupnik, M., Marhl, M., Stožer, A., et al. “Network science of biological systems at different scales: a review”. *Phys. Life Rev.*(2017)
- [49]. Gylfe, E., Grapengiesser, E., Dansk, H., and Hellman, B. “The neurotransmitter ATP<sup>2+</sup> triggers Ca Responses promoting coordination of pancreatic islet oscillations”. *Pancreas* 41, 258–263. (2012).